Astronomy
&
Astrophysics

WFPC2 observations of two dwarf spheroidal galaxies in the M 81 group[⋆]

I. D. Karachentsev[1], M. E. Sharina[1,10], A. E. Dolphin[2], D. Geisler[3], E. K. Grebel[4,6,⋆⋆],
P. Guhathakurta[5,⋆⋆⋆], P. W. Hodge[6], V. E. Karachentseva[7], A. Sarajedini[8], and P. Seitzer[9]

[1] Special Astrophysical Observatory, Russian Academy of Sciences, N. Arkhyz, KChR, 369167, Russia
[2] Kitt Peak National Observatory, National Optical Astronomy Observatories, PO Box 26732, Tucson, AZ 85726, USA
[3] Departamento de Fisica, Grupo de Astronomia, Universidad de Concepcion, Casilla 160-C, Concepcion, Chile
[4] Max-Planck-Institut für Astronomie, Königstuhl 17, 69117 Heidelberg, Germany
[5] UCO/Lick Observatory, University of California at Santa Cruz, Santa Cruz, CA 95064, USA
[6] Department of Astronomy, University of Washington, Box 351580, Seattle, WA 98195, USA
[7] Astronomical Observatory of Kiev University, 04053, Observatorna 3, Kiev, Ukraine
[8] Astronomy Department, Wesleyan University, Middletown, CT 06459, USA
[9] Department of Astronomy, University of Michigan, 830 Dennison Building, Ann Arbor, MI 48109, USA
[10] Isaac Newton Institute, SAO Branch Chile

Abstract. We have obtained HST WFPC2 and ground-based images of two low surface brightness dwarf spheroidal galaxies in the M 81 group, FM1 and KKH57. Their colour-magnitude diagrams show red giant branches with tips at $I = 23.77 \pm 0.14$ and $I = 23.97 \pm 0.17$, respectively. The derived true distance moduli, 27.66 ± 0.16 and 27.96 ± 0.19, agree well with the mean distance modulus of the M 81 group, 27.84 ± 0.05. Absolute V magnitudes of the galaxies (-11.46 and -10.85), their colours ($(B - V) = 0.88$ and 0.80), and central surface brightnesses ($\Sigma_{0,V} = 24.8$ and 24.4 mag/$\square''$) are in the range of other dSph companions of M 81, M 31, and Milky Way. With two new objects the maximum projected radius of the dwarf spheroidal subsystem around M 81 is 380 kpc.

Key words. galaxies: dwarf – galaxies: stellar content – galaxies: distances – galaxies: M 81 group: FM1 and KKH57

1. Introduction

The first three dwarf spheroidal galaxies in the M 81 group, DDO 44, DDO 71, and DDO 78, were discovered more than 40 years ago by van den Bergh (1959). In the following we call dwarf galaxies dwarf spheroidals (dSphs) if they are diffuse spheroidal objects with absolute V magnitudes of $M_V \gtrsim -14^{\rm m}$, surface brightnesses of $\Sigma_V \gtrsim 22$ mag arcsec^{-2}, and H I masses of $M_{\rm HI} \lesssim 10^5\ M_\odot$ (Grebel 2000). More recent studies (Karachentseva 1968; Börngen & Karachentseva 1982; Karachentsev 1994; Caldwell et al. 1998) have found six more dSphs around M 81 – K61, K64, BK5N, BK6N, KK77, and F8D1. All nine of these objects have been resolved into stars in Wide Field Planetary Camera 2 (WFPC2) images and confirmed as members of the M 81 group (Caldwell et al. 1998; Karachentsev et al. 1999; Karachentsev et al. 2000). In this paper we report observations with WFPC2 of two more dSph galaxies in the M 81 group: FM1 and KKH57. The former object was discovered by Froebrich & Meusinger (2000) on digitally stacked Schmidt telescope plates. The latter was found on POSS-II film copies by Karachentsev et al. (2001). Both galaxies are resolved into stars, yielding distances that are consistent with their membership in the M 81 group. As a result, the present number of known dSph systems in the
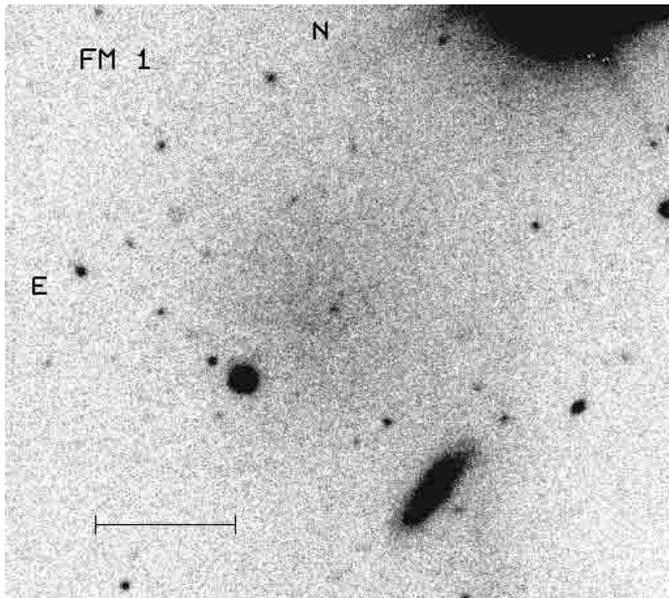
Fig. 1. V-band image of FM1 obtained with the 3.5 m APO telescope. The horizontal line indicates $30''$. North is up, and the east is to to the left.

Fig. 2. V-band image of KKH57 obtained with the 6 m SAO telescope. The arrows point to the north and east.

M 81 group has reached eleven, being comparable with the number of known dSph objects in the Local Group (van den Bergh 2000).

2. Ground-based observations

B, V CCD images of FM1 were obtained by E. Grebel and I. Karachentsev on February 3, 2000 using the 3.5 m APO telescope. Part of the V image, which was taken with $1''\!.5$ seeing and a 600 s exposure, is shown in Fig. 1. The galaxy is very diffuse, with a bright star to the northwest making photometry difficult. To the southwest is a background galaxy. Integrated photometry of FM1 has been performed by L. Makarova with increasing circular apertures. The sky level has been approximated by a two-dimensional polynomial, using regions with few stars near the edges of the images. The galaxy magnitude in each band has then been measured as the asymptotic value of the derived growth curve. The results are $B_{\mathrm{T}} = 17.50 \pm 0.15$ and $V_{\mathrm{T}} = 16.62 \pm 0.15$, values consistent with the photographic magnitudes $B_{\mathrm{T}} = 17.2$ and $R_{\mathrm{T}} = 15.9$ measured by Froebrich & Meusinger (2000).

KKH57 was observed in B and V with the APO telescope, as well as in V and I with the 6 m SAO (Russia) telescope on December 9, 1999. Figure 2 shows a 1200 s V image from the 6 m telescope. The galaxy looks more compact than FM1 and granulated because of the presence of stars near the detection threshold. Surface photometry of KKH57 obtained in the same manner as described above yields integrated magnitudes $B_{\mathrm{T}} = 17.86 \pm 0.15$ and $V_{\mathrm{T}} = 17.06 \pm 0.15$.
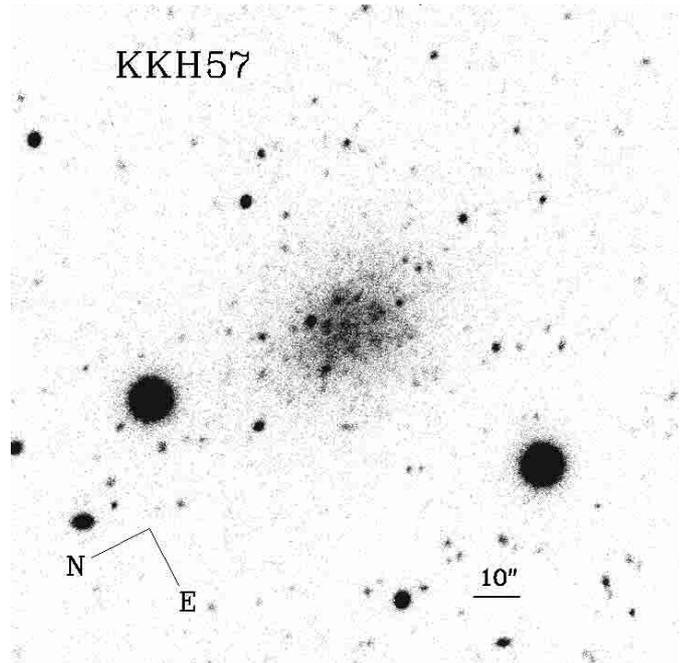
3. WFPC2 observations

Hubble Space Telescope WFPC2 observations of FM1 and KKH57 were obtained on July 8 and September 5, 2000, respectively, as part of the HST snapshot survey of probable nearby galaxies (program GO 8601, PI: P. Seitzer). Each galaxy was imaged in F606W and F814W with exposure times of 600 s each, with the galaxy centres located on the WFC3 chip. Figures 3 and 4 show the galaxy images resulting from the contribution of both filters to remove cosmic rays.

The photometric pipeline used for the snapshot survey has been described in detail in Dolphin et al. (2001), and what follows is only a summary. After obtaining the calibrated images from STScI, cosmic ray cleaning was made with the HSTphot (Dolphin 2000a) *cleansep* routine, which cleans images taken with different filters by allowing for a colour variation. Stellar photometry was then obtained with the HSTphot *multiphot* routine, which measures magnitudes simultaneously in the two images, accounting for image alignment, WFPC2's wavelength-dependent plate scale, and geometric distortion. The final photometry was then made using aperture corrections to a $0''\!.5$ radius, and the Dolphin (2000b) charge-transfer inefficiency correction and calibration applied. We estimate the aperture corrections in the three wide field chips to be accurate to 0.05 magnitudes. Because of the small sky coverage of the planetary camera (PC) and lack of stars for an accurate aperture correction, the PC photometry is omitted from our results. Additionally, stars with signal-to-noise <5, |chi| > 2.0, or |sharpness| > 0.4 in either exposure were eliminated from the final photometry list, in
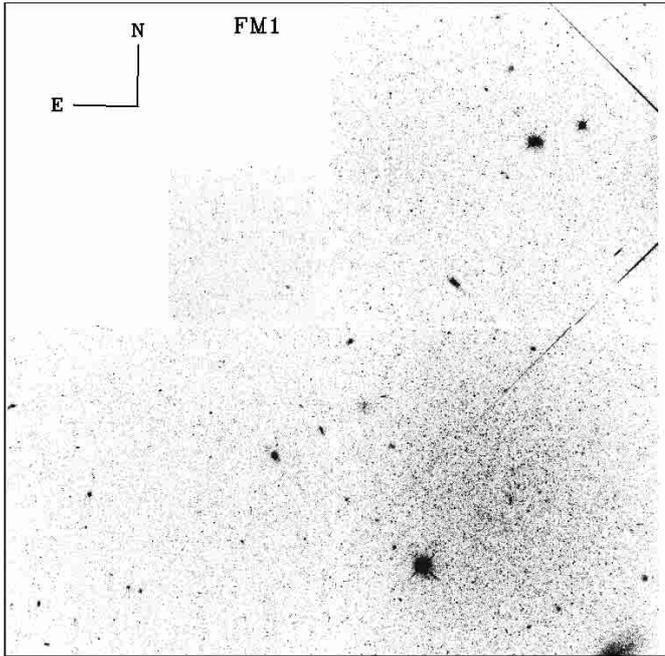
Fig. 3. WFPC2 image of FM1 produced by combining the two 600 s exposures taken through the F606W and F814W filters. The galaxy is centred in the WFC3 chip (WF3-FIX mode). North is up and east is to the left.
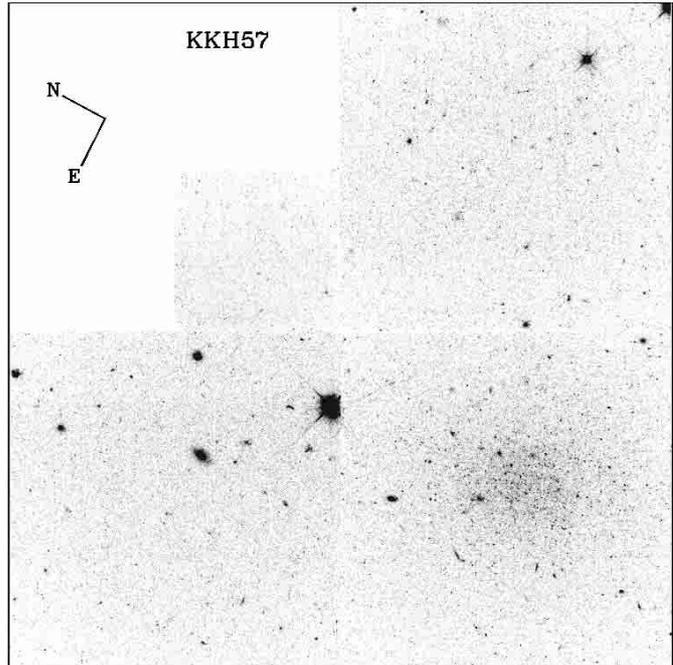

Fig. 4. WFPC2 image of KKH57 produced by combining the two 600 s exposures taken through the F606W and F814W filters. The galaxy is centred in the WFC3 chip. The arrows point to the north and east.

order to minimize the number of false detections. Finally, the F606W and F814W instrumental magnitudes were converted to the standard V, I system folowing the "synthetic" transformations of Holtzman et al. (1995). We used parameters of transformation from their Table 10 taking into account different relations for blue and red stars separately. Because we used the non-standard V filter F606W instead of F555W, the resulting I and especially V magnitudes may contain systematic errors. However, when comparing our F606W, F814W photometry of other snapshot targets with ground-based V, I photometry we find that the transformation uncertainties, σ_I and σ_{V-I}, are within $0.^{\mathrm{m}}05$ for stars with colors of $0 < (V - I) < 2$. The resulting $(V - I)$, I colour-magnitude diagrams (CMDs) are shown in Figs. 5 and 6.

We also measured integrated properties of the two galaxies using aperture photometry in circular apertures, finding $V_{\mathrm{T}} = 16.60 \pm 0.15$ and $I_{\mathrm{T}} = 15.21 \pm 0.15$ for FM1 and $V_{\mathrm{T}} = 17.00 \pm 0.15$ and $I_{\mathrm{T}} = 15.82 \pm 0.15$ for KKH57, as well as the central surface brightness and the exponential scale length presented in Table 1.

4. Colour-magnitude diagrams and distances

In Figs. 5 and 6 the left panels show the CMDs for the central WFC3 fields covering the main galaxy bodies. The middle panels represent the CMD for the neighbouring halves of WFC2 and WFC4 ($x < 425$ in WFC2 and $y < 425$ in WFC4), and the right panels are comprised of stars found in the remaining outer halves of WFC2 and

Table 1. Properties of two new dSph galaxies in the M 81 group.

| Parameter	FM1	KKH57
RA (2000.0)	$09^{\mathrm{h}}45^{\mathrm{m}}10\overset{\mathrm{s}}{.}0$	$10^{\mathrm{h}}00^{\mathrm{m}}16\overset{\mathrm{s}}{.}0$
Dec (2000.0)	$+68°45'54''$	$+63°11'06''$
$E(B-V)$	0.08	0.02
A_V	0.24	0.07
A_I	0.14	0.04
$a \times b$, (′)	0.9×0.8	0.6×0.5
V_{T}	16.62 ± 0.15	17.06 ± 0.15
$(B-V)_{\mathrm{T}}$	0.88 ± 0.15	0.80 ± 0.15
$(V-I)_{\mathrm{T}}$	1.39 ± 0.15	1.18 ± 0.15
$\Sigma_{0,V}$	24.8 ± 0.2	24.4 ± 0.2
h, (″)	21	14
$I(\mathrm{TRGB})$	23.77 ± 0.14	23.97 ± 0.16
μ_0	27.66 ± 0.17	27.96 ± 0.19
$(V-I)_{0,-3.5}$	1.37 ± 0.05	1.42 ± 0.05
[Fe/H]	-1.6 ± 0.6	-1.4 ± 0.6
[Fe/H] (CG97)	-1.3 ± 0.6	-1.2 ± 0.6
$D_{26.5}$, kpc	0.97	0.64
M_V	-11.46	-10.85
$r(\mathrm{M\ 81})$, (′)	59	354
$R(\mathrm{M\ 81})$, kpc	64	381
Type	dSph	dSph
N_{gc}	0	0
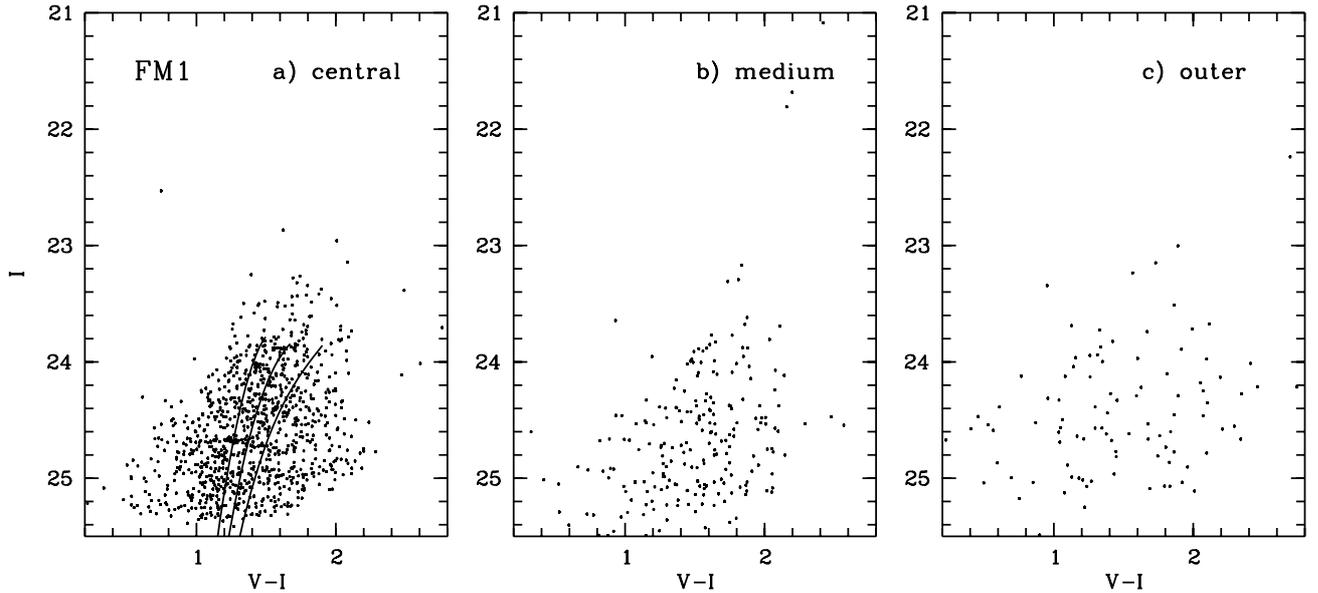
Fig. 5. WFPC2 colour-magnitude diagram for the dSph galaxy FM1. The left panel shows stars in WFC3 (the center of the galaxy), the middle panel the "medium" field (neighbouring halves of the WFC2 and WFC4 chips), and the right panel the "outer" field (remaining halves of the WFC2 and WFC4 chips). Each of these three fields covers an equal area of 750×750 pixels. The solid lines in the left panel show the red giant branches of globular clusters with different metallicities: M 15 (-2.17 dex), M 2 (-1.58 dex), and NGC 1851 (-1.29 dex).
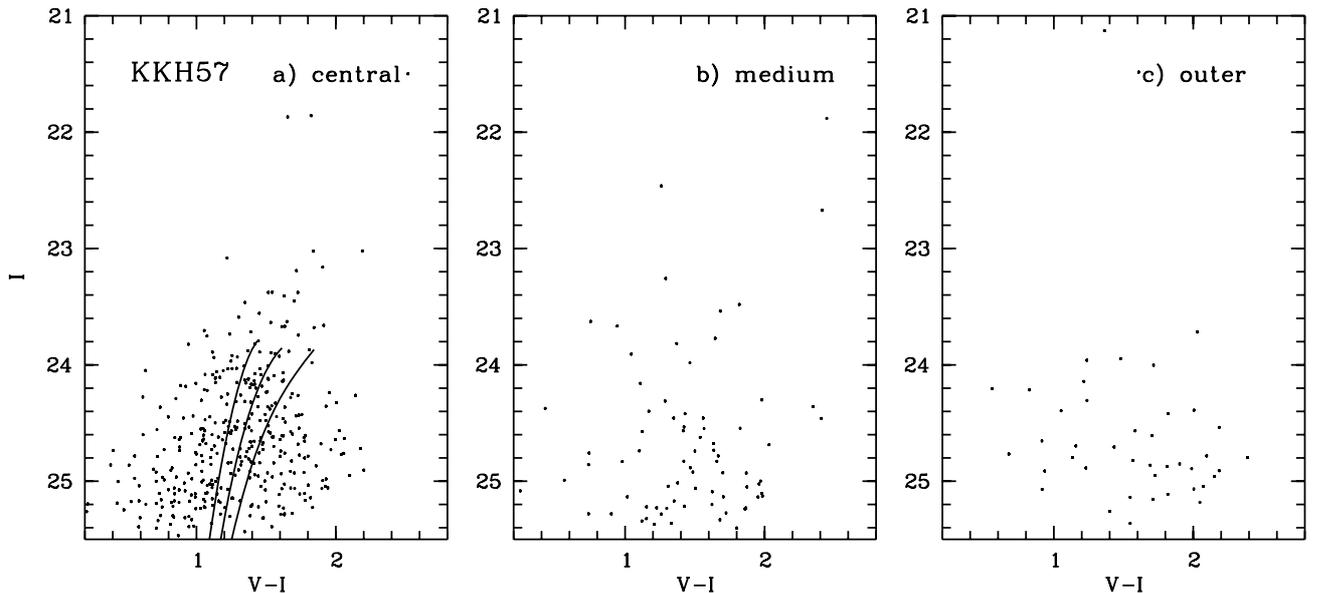

Fig. 6. WFPC2 colour-magnitude diagram for the dSph galaxy KKH57, displayed as in Fig. 5.

WFC4. As seen from these CMDs, the observed stellar populations of both galaxies consist predominately of red stars. To measure the distances to these galaxies, we apply the red giant branch (RGB) tip method described by Lee et al. (1993). The Gaussian-smoothed I-band luminosity functions for the central fields of FM1 and KKH57 are shown in the top panels of Fig. 7. Only red stars with colors $1 < (V - I) < 2$ were considered. Measurement the RGB tip positions can be done using a Sobel filter.

Following Sakai et al. (1996), we apply an edge-detection filter, which is a modified version of a Sobel kernel ($[-1,0, +1]$), to the luminosity functions to determine objectively the positions of the TRGB. The results of convolution are shown in the bottom panels of Fig. 7. The positions of the TRGB are identified with the highest peak in the filter output function. For FM1 and KKH57 we obtain $I_{\rm TRGB} = 23.77 \pm 0.14$ and 23.97 ± 0.16, respectively. Artificial star tests were also made, so that the accuracy
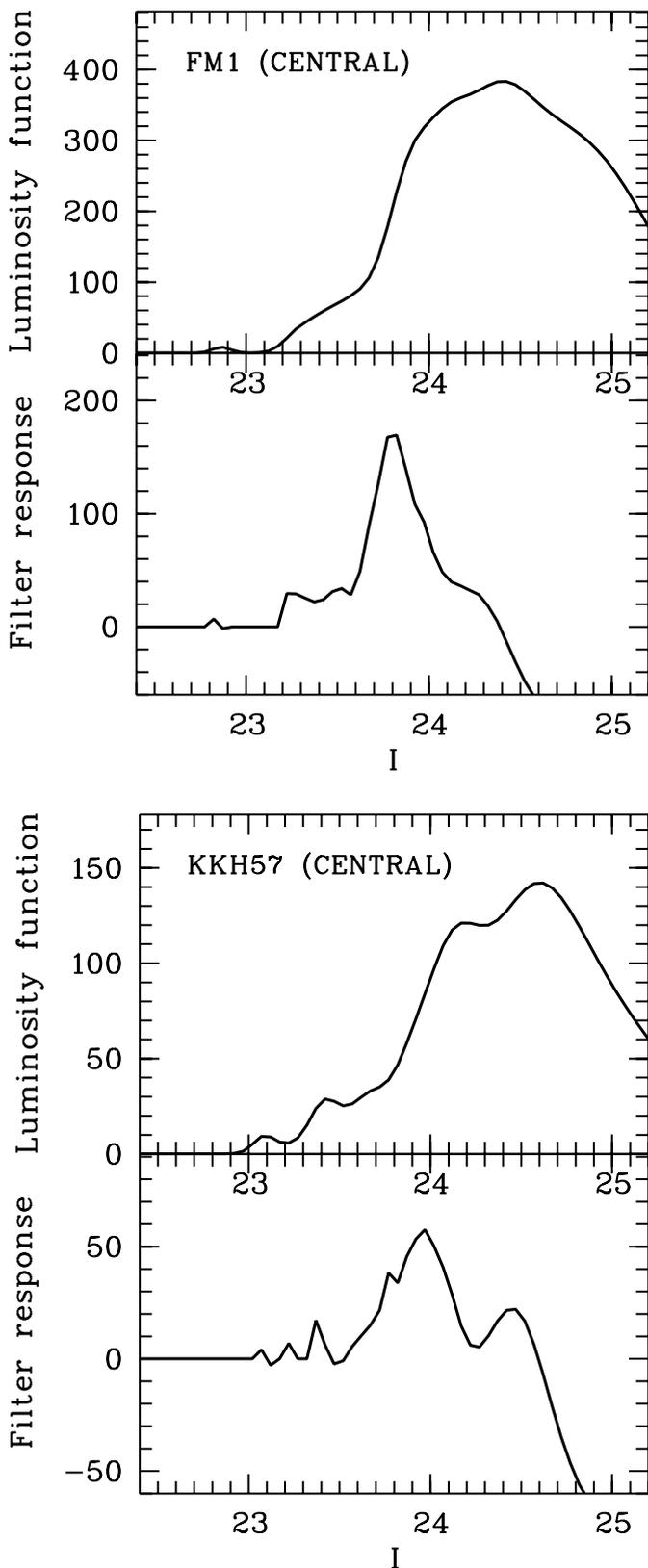
Fig. 7. The Gaussian-smoothed I-band luminosity function restricted to red stars with colors between $1 < (V - I) < 2$ (top), and output of an edge-detection filter applied to the luminosity function (bottom) for FM1 and KKH57. The position of the TRGB is indicated by the highest peak in the output functions.

and completeness of the crowded WF3 photometry could be measured. We can conclude from these simulations that the detection rate dropped to 50% at $I_{\mathrm{lim}} = 24.8$ and $V_{\mathrm{lim}} = 25.9$. The scatter of colors and magnitudes for the detected stars increases towards faint magnitudes. At the level of $I \sim 23\overset{\mathrm{m}}{.}8$ the position of the TRGB shifts to a brighter ($0\overset{\mathrm{m}}{.}06$) and bluer ($0\overset{\mathrm{m}}{.}04$) magnitude due to stellar crowding. The same effect has been shown by Madore & Freedman (1995).

Adopting an RGB tip absolute magnitude of $M_I = -4.03 \pm 0.05$ estimated from the theoretical models of Girardi et al. (2000) and the semi-empirical calibration of Lee et al. (1993) and Galactic extinction values of $A_I = 0.14$ (FM1) and $A_I = 0.04$ (KKH57), calculated from the maps of Schlegel et al. (1998), we derive distance moduli of $\mu_0 = 27.66 \pm 0.17$ and $\mu_0 = 27.96 \pm 0.19$, respectively. The quoted errors include the error in the TRGB detection, and also uncertainties of the HST photometry zero point ($\sim 0\overset{\mathrm{m}}{.}05$), the aperture corrections ($\sim 0\overset{\mathrm{m}}{.}05$), and crowding effects ($\sim 0\overset{\mathrm{m}}{.}06$) added in quadrature.

Three solid lines in the left panels of Figs. 5 and 6 are globular cluster fiducials from Da Costa & Armandroff (1990), adjusted for the reddening and distance of each galaxy. The fiducials cover the range of metallicity values [Fe/H] = -2.17 dex for M 15, -1.58 dex for M 2, and -1.29 dex for NGC 1851 (from left to right).

5. Integrated properties

Table 1 presents a summary of basic properties of FM1 and KKH57 in the same format as for eight previously-considered dSphs in the M 81 group (Karachentsev et al. 2000). Its lines contain: (1, 2) equatorial coordinates, (3–5) Galactic extinction from Schlegel et al. (1998), (6) galaxy dimensions along the major and minor axes approximately corresponding to a level of $B = 26.5$ mag/$\square''$, (7) integrated V magnitude, (8, 9) integrated colours, (10) observed central surface brightness, (11) exponential scale length in arcsec averaged over the V and I bands, (12) apparent I magnitude of the RGB tip, (13) true distance modulus, (14, 15) mean reddening-corrected colour of the RGB tip measured at an absolute magnitude $M_I = -3.5$, as recommended by Lee et al. (1993) and corresponding mean metallicity, (16) mean metallicity on the scale of Carretta & Gratton (1997), (where the errors were calculated by carying the color uncertainty into the Lee et al. formula, as well as the intrinsic uncertainty in such a calibration, and the difference between the metallicity scales is discussed at length by Carretta & Gratton 1997), (17, 18) linear diameter and total absolute magnitude of the galaxy with the mean distance modulus of 27.84, (19, 20) angular and linear projected separation of the galaxy from M 81, (21) morphological type, and (22) number of globular cluster candidates in each galaxy.

6. Discussion

Froebrich & Meusinger (2000) imaged FM1 in the H_α line, finding no indication of significant H_α emission. Karachentsev et al. (2001) observed KKH57 in the 21 cm line with the 100-m Effelsberg telescope and obtained an upper limit of the H I flux of 5 mJy, corresponding to an H I mass limit of 4×10^5 solar masses. This limit is similar to the upper H I mass limit found for Local Group dSphs. The symmetric shape of both galaxies, their smooth surface brightness profiles, the reddish integrated colours, the lack of an appreciable amount of hydrogen, and the absence of a population of bright blue stars (see Figs. 5 and 6) favour the classification of FM1 and KKH57 as dSph galaxies.

According to the summary of distance moduli for 11 members of the M 81 group (Table 4 in Karachentsev et al. 2000) measured via the RGB tip or Cepheids, the mean distance modulus of the group is 27.84 ± 0.05. Therefore, the distance moduli of these two new dSph galaxies, 27.66 ± 0.17 and 27.96 ± 0.19, are consistent with their membership in that group.

Judging by the absolute V-band magnitudes (-11.46 and -10.85) and linear diameters (0.97 kpc and 0.64 kpc), FM1 and KKH57 are among the faintest known dSph members of the M 81 group. Nevertheless, their luminosities exceed by about two magnitudes the luminosity of the faintest dSphs in the Local Group: Draco (-8.6), Ursa Minor (-8.9), and Andromeda V (-9.1). It is quite likely that similar systems exist in the M 81 group as well, but have not yet been detected. (Two new extremely low surface brightness objects of the dSph type were found in the M 81 group by Karachentseva and Karachentsev in December 2000.) The presence of Galactic cirrus in that direction (Sandage 1976) makes such a search extremely difficult. The Local Group contains 10 dSphs with absolute magnitudes brighter than $M_V = -10^{\mathrm{m}}$, very similar in number to the 11 dSphs currently known down to this magnitude limit in the M 81 group. The Local Group contains at least seven dSphs fainter than $M_V = -10^{\mathrm{m}}$, which lets near-infrared searches for faint extended objects in the M 81 group appear a promising approach to detect additional, faint dwarf members.

Figure 8 shows the positions of ten dSph companions of M 81 in equatorial coordinates. The most remote companion, KKH57, has a projected distance of 381 kpc from M 81. The distribution of dSphs looks to be asymmetric, which can be caused by the presence of Galactic cirrus in the M 81 group direction.

We searched for globular clusters in FM1 and KKH57 but found no candidates with the appropriate range of colours, magnitudes and half-light radii defined by Milky Way globulars. This null result is not surprising, given the low expected value of the specific frequency of globular clusters in low-luminosity dSphs (Miller et al. 1998) – the presence of even one globular in FM1 (the brighter of the two) would produce a specific frequency S_N of nearly 30,
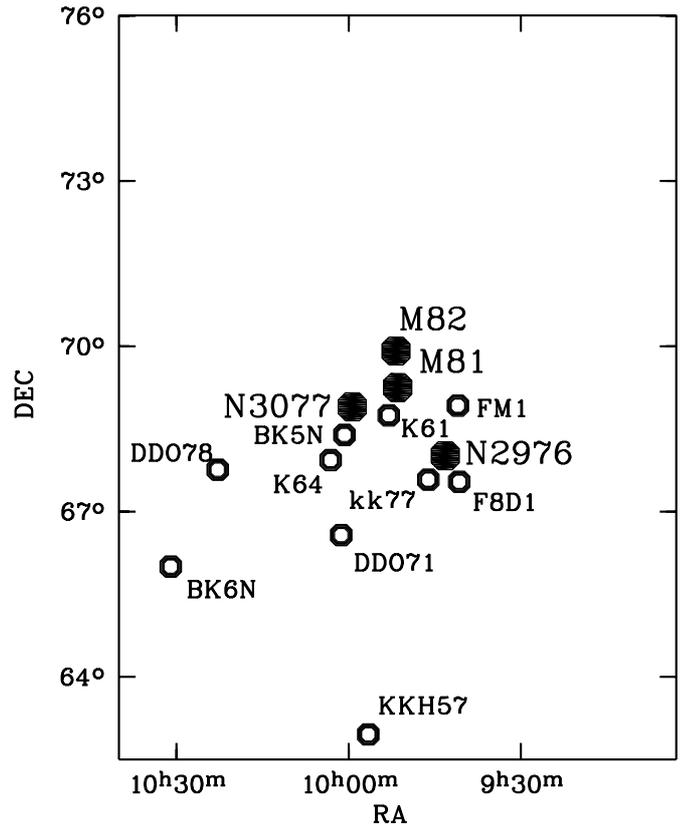

Fig. 8. The distribution of dSph galaxies in equatorial coordinates around M 81. The four bright galaxies are indicated with large filled circles; dwarf spheroidals are indicated with small open circles. The asymmetric distribution of dSphs can be caused by the presence of Galactic cirrus in the M 81 group direction.

much larger than any galaxy in the Miller et al. (1998) sample.

References

Börngen, F., & Karachentseva, V. E. 1982, Astron. Nachr., 303, 189
Caldwell, N., Armandroff, T. E., Da Costa, G. S., & Seitzer, P. 1998, AJ, 115, 535
Carretta, E., & Gratton, R. G. 1997, A&AS, 121, 95
Da Costa, G. S., & Armandroff, T. E. 1990, AJ, 100, 162
Dolphin, A. E. 2000a, PASP, 112, 1383

Dolphin, A. E. 2000b, PASP, 112, 1397

Dolphin, A. E., Makarova, L., Karachentsev, I. D., et al. 2001, MNRAS, in press

Froebrich, D., & Meusinger, H. 2000, A&A, 145, 229

Girardi, L., Bressan, A., Bertelli, G., & Chiosi, C. 2000, A&AS, 141, 371

Grebel, E. K. 2000, 33rd ESLAB Symposium on Star Formation from the Small to the Large Scale, SP-445, ed. F. Favata, A. A. Kaas, & A. Wilson (Noordwijk: ESA), 87

Holtzman, J. A., Burrows, C. J., Casertano, S., et al., 1995, PASP, 107, 1065

Karachentsev, I. D. 1994, Astron. Astrophys. Trans., 6, 1

Karachentsev, I. D., Sharina, M. E., Grebel, E. K., et al. 1999, A&A, 352, 399

Karachentsev, I. D., Karachentseva, V. E., Dolphin, A. E., et al. 2000, A&A, 363, 117

Karachentseva, V. E. 1968, Commun. Byurakan obs. 39, 62

Karachentsev, I. D., Karachentseva, V. E., & Huchtmeier, W. K. 2001, A&A, 366, 428

Lee, M. G., Freedman, W. L., & Madore, B. F. 1993, ApJ, 417, 553

Madore, B. F., & Freedman, W. L. 1995, AJ, 109, 1645

Miller, B. W., Lotz, J. M., Ferguson, H. C., Stiavelli, M., & Whitmore, B. C. 1998, ApJ, 508, L133

Sakai, S., Madore, B. F., & Freedman, W. L. 1996, ApJ, 461, 713

Sandage, A. R. 1976, AJ, 81, 964

Schlegel, D. J., Finkbeiner, D. P., & Davis, M. 1998, ApJ, 500, 525

van den Bergh, S. 1959, Publ. of D.D.O., II, (5), 147

van den Bergh, S. 2000, The Galaxies of the Local Group (Cambridge University Press)